Journal of Solid State Chemistry 185 (2012) 187–190

Contents lists available at SciVerse ScienceDirect

Journal of Solid State Chemistry

journal homepage: www.elsevier.com/locate/jssc

Photoluminescence properties of rare earths (Eu^{3+}, Tb^{3+}, Dy^{3+} and Tm^{3+}) activated $NaInW_2O_8$ wolframite host lattice

S. Asiri Naidu [a], S. Boudin [a], U.V. Varadaraju [b], B. Raveau [a,*]

[a] Laboratoire de Cristallographie et Sciences des Matériaux, ENSICAEN, Université de Caen, CNRS, 6 Bd Maréchal Juin, F-14050 Caen, France
[b] Department of Chemistry, Indian Institute of Technology Madras, Chennai 600036, India

ARTICLE INFO

Article history:
Received 3 August 2011
Received in revised form
19 October 2011
Accepted 22 October 2011
Available online 29 October 2011

Keywords:
$NaInW_2O_8$
Photoluminescence
Energy transfer
Host absorption

ABSTRACT

The photoluminescence (PL) studies on $NaIn_{1-x}RE_xW_2O_8$, with $RE=Eu^{3+}$, Tb^{3+}, Dy^{3+} and Tm^{3+} phases have shown that the relative contribution of the host lattice and of the intra-*f*–*f* emission of the activators to the PL varies with the nature of the rare earth cation. In the case of Dy^{3+} and Tm^{3+} activators, with yellow and blue emission, respectively, the energy transfer from host to the activator plays a major role. In contrast for Eu^{3+}, with intense red emission, the host absorption is less pronounced and the intra-*f*–*f* transitions of the Eu^{3+} ions play a major role, whereas for Tb^{3+} intra-*f*–*f* transitions are only observed, giving rise to green emission.

1. Introduction

The PL properties of rare earth doped phosphors depend strongly on the nature of the host lattice. Therefore, it is important to understand the behavior of rare earth ions w.r.t. the PL properties in various host lattices. Such studies are essential to understand energy transfer processes from a fundamental point of view, in order to discover and to develop new phosphor materials for applications. Ln^{3+} ions exhibit a range of emission colors based on 4*f*–4*f* or 5*d*–4*f* transitions [1] and have been playing an important role in solid state lighting and other display devices. The *f*–*f* transitions in Ln^{3+} ions have low excitation efficiencies because of the forbidden parity selection rules. So, energy transfer from another efficient absorber to the Ln^{3+} ions is very crucial in enhancing the luminescence efficiency of Ln^{3+} ions. Host sensitization of Ln^{3+} ions is an important route to realize efficient emission of Ln^{3+} ions, e.g., YVO_4:Eu^{3+}, $CaIn_2O_4$:Dy^{3+} and $SrIn_2O_4$:Dy^{3+} [2–4]. Double tungstates activated with rare-earth ions have drawn a notably large interest in the field of solid state lighting, solid-state lasers and inorganic scintillation applications [5–12]. The main reason for this is due to their efficient radiative emissions in the visible and mid-infrared spectral regions. Interestingly, the double tungstate $LiInW_2O_8$ with the wolframite structure (monoclinic *C*2/*c*), was recently shown to be a promising phosphor for solid state applications, when doped or co-doped with various rare earth ions such as Tm^{3+} (blue), Dy^{3+} (white) Eu^{3+} (red) as and Eu^{3+}/Dy^{3+} (white) [13,14]. The PL properties of rare earth activated $NaInW_2O_8$ wolframite series have not been explored.

With this view, in the present study, we have explored the PL properties of Eu^{3+}, Tb^{3+}, Dy^{3+} and Tm^{3+} doped $NaInW_2O_8$ host lattice. We show the intense characteristic emissions of the rare earth ions in $NaInW_2O_8$ and we compare these phosphors with those derived from the isotypic $LiInW_2O_8$ host lattice recently reported [14].

2. Experimental

$NaIn_{1-x}RE_xW_2O_8$ ($x=0.01$, 0.03, 0.05, 0.06, 0.07, 0.1; $RE=Eu^{3+}$, Tb^{3+}, Dy^{3+} and Tm^{3+}), $LiInW_2O_8$ and $LiIn_{0.95}Tb_{0.05}W_2O_8$ phases were prepared by solid state reaction as reported in the literature [13,15]. The starting materials used were Li_2CO_3 (99%, Aldrich), Na_2CO_3 (99%, Aldrich), In_2O_3 (99.9%, Alfa Aesar), WO_3 (99.8%, Alfa Aesar), Eu_2O_3, Tb_7O_{12}, Dy_2O_3 and Tm_2O_3 (99.9%, Alfa Aesar). Eu_2O_3, Tb_7O_{12}, Dy_2O_3 and Tm_2O_3 were preheated at 900 °C overnight in air. Stoichiometric amounts of the reactants were intimately ground, placed in a platinum crucible and heated at 700 °C for 15 h and 900 °C for 48 h in air. The synthesis conditions for $LiInW_2O_8$ were: 700 °C for 15 h and 950 °C for 15 h in air.

Powder X-ray diffraction data were recorded for all the above samples using a Panalytical X'pert Pro X-ray diffractometer with a Cu*K*α1 source ($\lambda=1.5418$ Å). Diffuse reflectance spectra were recorded using a CARY 100 Varian spectrophotometer over the spectral range of 200–800 nm. $BaSO_4$ was used as a reference for

* Corresponding author. Fax: +33 2 31 95 16 00.
E-mail address: bernard.raveau@ensicaen.fr (B. Raveau).

0022-4596/$ - see front matter © 2011 Elsevier Inc. All rights reserved.
doi:10.1016/j.jssc.2011.10.035

100% reflectance. Excitation and emission spectra were recorded using a Fluorolog-3 Horiba Jobin Yvon spectrofluorometer equipped with a 450 W Xenon lamp. All the measurements were carried out at room temperature.

3. Results and discussion

3.1. Structural analysis of $NaInW_2O_8$

$NaInW_2O_8$, isostructural with $NaFeW_2O_8$ and crystallizes in the monoclinic wolframite structure with $P2/c$ symmetry [16]. In this crystal structure, the WO_6 octahedra share edges forming $[WO_4]_\infty$ zig-zag chains along the c-direction (Fig. 1). The InO_6 octahedra, share apices with the WO_6 octahedra, ensuring connectivity between the $[WO_4]_\infty$ chains. The Na^+ ions are octahedrally coordinated to oxide ions and are located in tunnels formed by $[WO_4]_\infty$ chains and InO_6 octahedra, running along c-axis. The powder XRD patterns of $NaIn_{0.93}Eu_{0.07}W_2O_8$ and $NaInW_2O_8$ phases are shown in Fig. 2. All the diffraction peaks of $NaIn_{1-x}RE_xW_2O_8$ ($0 \le x \le 0.05$) phases can be indexed on the basis of a monoclinic cell with space group $P2/c$. For compositions with $x \ge 0.07$, unidentified peaks with weak intensity appear at the diffraction angles: $2\theta = 18.78^\circ$ and 32.27°, for all the rare earth doped phases. A similar observation was made in the case of $LiInW_2O_8$:0.1Tm phase reported recently [13].

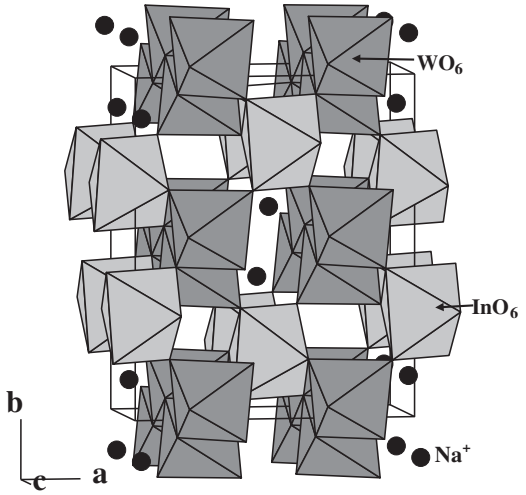

Fig. 1. $NaInW_2O_8$ crystal structure (WO_6 and InO_6 octahedra are represented in dark and light gray, respectively, Na^+ ions with black balls).

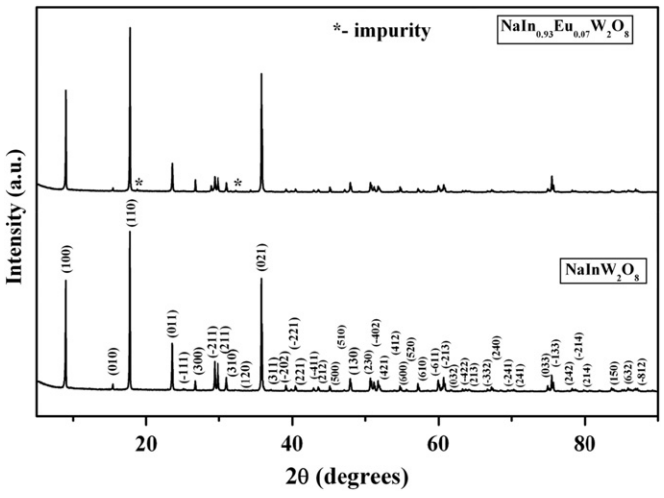

Fig. 2. X-Ray powder diffraction patterns of $NaInW_2O_8$ and $NaIn_{0.93}Eu_{0.07}W_2O_8$ phases.

3.2. Diffuse reflectance spectroscopy

The diffuse reflectance spectrum of $NaInW_2O_8$ is very similar to that of $LiInW_2O_8$ (Fig. 3). The optical band gap values are calculated from the absorption onsets as shown by Tandon and Gupta [17]. The measured band gap values are 3.66 and 3.85 eV for $NaInW_2O_8$ and $LiInW_2O_8$, respectively.

3.3. Photoluminescence properties

The PL excitation spectrum of $NaInW_2O_8$ ($\lambda_{em} = 460$ nm) (Fig. 4a) shows a maximum at 309 nm. The origin of the blue emission in such a host lattice can be due to transitions within the InO_6 and/or WO_6. Indeed, blue luminescence under UV irradiation has previously been observed either in pure tungstate matrices such as $KLu(WO_4)_2$ and $AgLa(WO_4)_2$ [18,19] or in pure indate matrices such as $LaInO_3$, $CaIn_2O_4$ or $SrIn_2O_4$ [3–4,20]. The WO_6 octahedra play a major role in the blue emission of both,

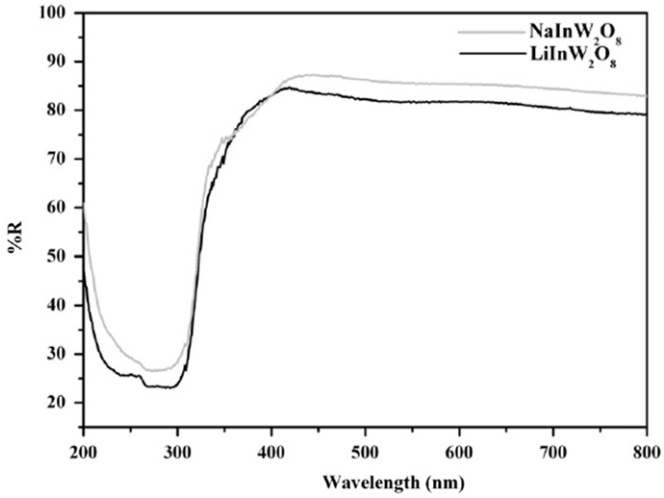

Fig. 3. Diffuse reflectance spectra of $NaInW_2O_8$ and $LiInW_2O_8$.

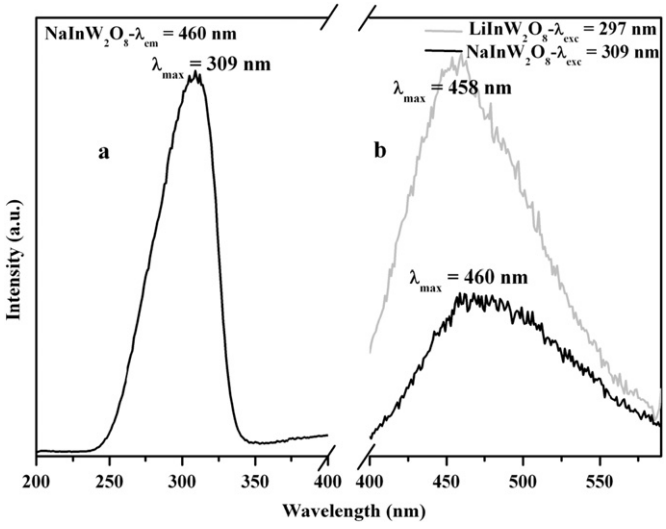

Fig. 4. Excitation spectrum of $NaInW_2O_8$ and comparative emission spectra of $NaInW_2O_8$ and $LiInW_2O_8$.

$LiInW_2O_8$ and $LiScW_2O_8$ recently reported [14]. In a similar way, in the present study, WO_6 octahedra play a major role in the blue emission of $NaInW_2O_8$. The intrinsic luminescence of the tungstate is due to the $^3T_1$ and $^3T_2 \rightarrow {}^1A_1$ spin-forbidden electronic transitions [21]. Furthermore, a comparison of the emission intensities of $LiInW_2O_8$ and $NaInW_2O_8$ hosts (Fig. 4b) shows that the emission intensity of the $LiInW_2O_8$ host lattice is higher than that of $NaInW_2O_8$, though, the WO_6 octahedra are more distorted in $NaInW_2O_8$, compared to $LiInW_2O_8$ as shown from the comparison of the interatomic distances (Table 1) [16,14].

Fig. 5a shows the excitation spectrum of $NaIn_{0.95}Eu_{0.05}W_2O_8$ (λ_{em}=615 nm). The excitation spectrum consists of a broad band in the range 200–350 nm with a maximum at 309 nm and is attributed to the host lattice absorption (Fig. 4a). The Eu^{3+}–O^{2-} charge transfer band (CTB) is not conspicuous in the excitation spectrum, probably due to overlap with the host absorption band. The peaks at 395 ($^7F_0 \rightarrow {}^5L_6$) and 465 nm ($^7F_0 \rightarrow {}^5D_2$) are due to the intra-*f*–*f* electronic transitions of the Eu^{3+} ion. The $^7F_0 \rightarrow {}^5L_6$ transition at 395 nm excitation is predominant among all the transitions in the excitation spectrum. In the case of $LiInW_2O_8$:Eu^{3+}, the host absorption at 297 nm is the dominant one among all the transitions observed from the excitation spectrum [14], though, both host lattices belong to the same wolframite family. The emission spectrum of $NaIn_{0.95}Eu_{0.05}W_2O_8$ phase under 395 nm is shown in Fig. 5b. The emission spectrum consists of groups of lines between 575 and 700 nm corresponding to $^5D_0 \rightarrow {}^7F_J$ (J=0–4) transitions of Eu^{3+} [22]. The $^5D_0 \rightarrow {}^7F_2$ electric dipole transition at 615 nm is dominant, which reveals that the site occupied by Eu^{3+} has no inversion center.

Table 1
Interatomic bond distances (Å) of $NaInW_2O_8$ [16] and $LiInW_2O_8$ [14] compounds.

W–O(1)	1.98	W–O(1)	1.84
W–O(1)	2.16	W–O(2)	1.72
W–O(2)	1.79	W–O(3)	1.88
W–O(3)	1.84	W–O(4)	1.90
W–O(3)	2.07	W–O′(3)	2.09
W–O(4)	1.81	W–O′(4)	2.24
W–O	1.94	W–O	1.94
In–O(1)	2.10 × 2	In–O(1)	2.16 × 2
In–O(2)	2.08 × 2	In–O′(1)	2.31 × 2
In–O(4)	2.23 × 2	In–O(4)	2.11 × 2
In–O	2.14	In–O	2.19
Li–O(2)	2.37 × 2	Na–O(2)	2.25 × 2
Li–O(3)	2.15 × 2	Na–O′(2)	2.42 × 2
Li–O(4)	2.07 × 2	Na–O′(3)	2.39 × 2
Li–O	2.19	Na–O	2.35

The excitation spectrum of $NaIn_{0.95}Dy_{0.05}W_2O_8$ (λ_{em}=579 nm) (Fig. 6a) consists of a strong excitation band between 200 and 350 nm with a maximum at 309 nm, due to the host absorption. The weak transitions in the longer wavelength region are due to the $4f^9$–$4f^9$transitions of the Dy^{3+} cation [1]. In the case of Eu^{3+} doped phases, the Eu^{3+}–O^{2-} charge transfer absorption band is located in the UV region. This is not the case for Dy^{3+}; the charge transfer band of Dy^{3+} is located below 200 nm [23] and Dy^{3+} can be excited only with forbidden *f*–*f* transitions. Hence, the Dy^{3+} emission can be enhanced by host sensitization or by co-doping of a sensitizer ion. The emission spectrum of Dy^{3+} in $NaIn_{0.95}Dy_{0.05}W_2O_8$ under host excitation (309 nm) shows narrow bands with λ_{max} at 487 nm ($^4F_{9/2} \rightarrow {}^6H_{15/2}$, blue) and 579 nm ($^4F_{9/2} \rightarrow {}^6H_{13/2}$, yellow) (Fig. 6b). It is known that the 487 nm (blue) band ($^4F_{9/2} \rightarrow {}^6H_{15/2}$) is due to the magnetic dipole transition and the 579 nm (yellow) band ($^4F_{9/2} \rightarrow {}^6H_{13/2}$) is due to the electric dipole transition. $^4F_{9/2}$–$^6H_{13/2}$ is dominant only when the Dy^{3+} ions occupy sites, with no inversion centers [24]. This corroborates well with the reported structural features, viz., distorted InO_6 octahedra (Table 1). In the case of $LiInW_2O_8$:Dy^{3+}, the emission spectra consist of bands due to host lattice as well as Dy^{3+} emission, under host lattice excitation. Thus, the whole region from 450 to 650 nm is covered resulting in white light generation [14]. However, in the present study, under host excitation, a very weak band due to the host lattice is observed and the emission color of $NaIn_{0.95}Dy_{0.05}W_2O_8$ is yellow and is due to Dy^{3+}. Thus, it can be concluded that the host emission is almost quenched when doped with Dy^{3+}. It is possible that the energy transfer to Dy^{3+} from the host is more efficient in this lattice vis a vis the Li containing phases. In both cases, viz., $NaInW_2O_8$:Dy^{3+}, $LiInW_2O_8$:Dy^{3+} the host lattice absorption band is dominant from the excitation spectra.

The excitation and emission spectra of $NaIn_{0.95}Tm_{0.05}W_2O_8$ are shown in Fig. 7a and b. The dominant emission band at 483 nm ($^1D_2 \rightarrow {}^3F_4$) is observed under host lattice excitation (309 nm). A similar result has been reported recently in the $LiIn_{1-x}Tm_xW_2O_8$ host lattice with the wolframite structure [13].

The excitation and emission spectra of $NaIn_{0.95}Tb_{0.05}W_2O_8$ are shown in Fig. 8a and b. No absorption corresponding to the host is observed in the excitation spectra. The broad band observed in the 240–300 nm range is attributed to $4f^8$–$4f^75d^1$ transition.

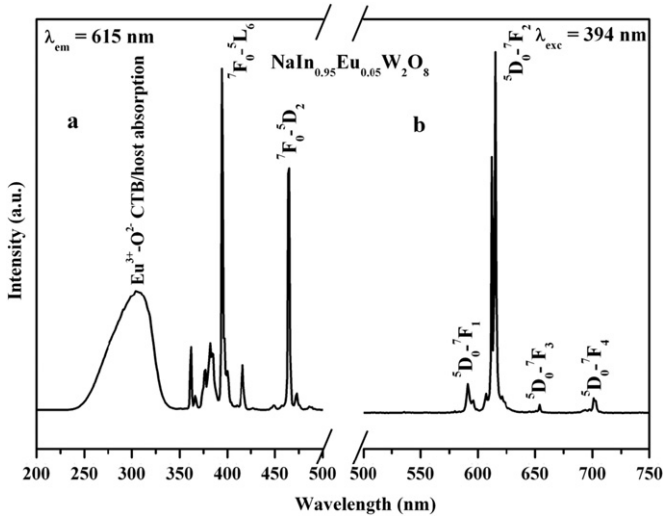

Fig. 5. Excitation and emission spectra of $NaIn_{0.95}Eu_{0.05}W_2O_8$.

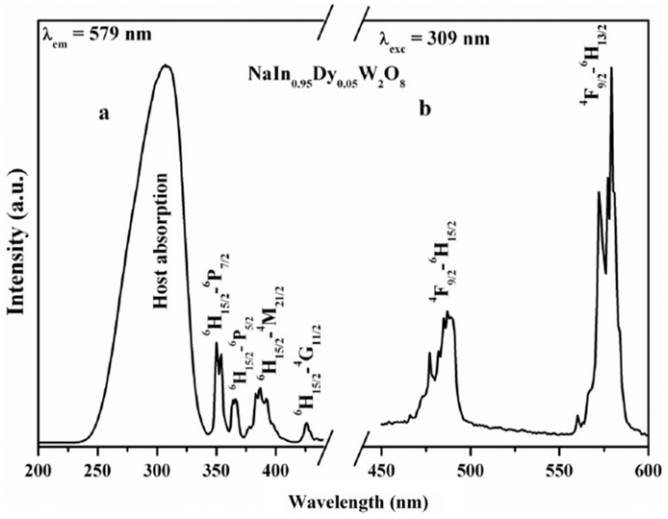

Fig. 6. Excitation and emission spectra of $NaIn_{0.95}Dy_{0.05}W_2O_8$.

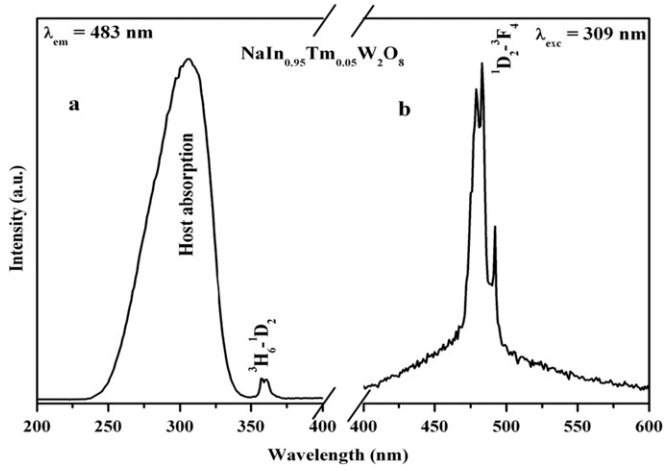

Fig. 7. Excitation and emission spectra of $NaIn_{0.95}Tm_{0.05}W_2O_8$.

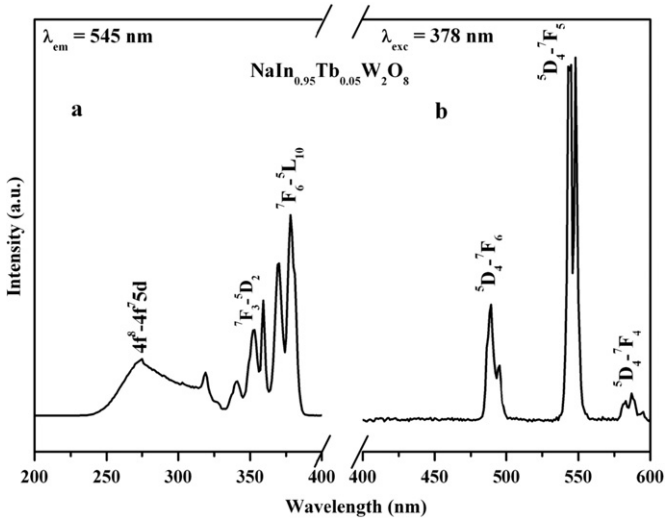

Fig. 8. Excitation and emission spectra of $NaIn_{0.95}Tb_{0.05}W_2O_8$.

The observed excitation bands in the 310–400 nm correspond to intra-4*f*–4*f* transitions of Tb^{3+} [25]. The emission spectrum consists of transitions at 485 ($^5D_4 \rightarrow {}^7F_6$), 550 ($^5D_4 \rightarrow {}^7F_5$), 585 nm ($^5D_4 \rightarrow {}^7F_4$) and the 550 nm transition is the predominant one. For comparison, we synthesized the Tb^{3+} doped analog, viz., $LiIn_{0.95}Tb_{0.05}W_2O_8$ in the present study. In contrast to the green emission observed in the case of $NaIn_{0.95}Tb_{0.05}W_2O_8$, no emission corresponding to Tb^{3+} is observed for the $LiIn_{0.95}Tb_{0.05}W_2O_8$ phase. From all the above observations made from the PL studies, it is clear that minor structural variations in the host lattice play an important role in determining the luminescence properties of rare earth ions.

Variation in the concentration of activator ions can influence the emission of a phosphor. Generally, a low concentration of activator ion gives weak emission, but high concentrations of activator ion can cause quenching of emission. In the present study, the critical concentration is found to be $x=0.05$ for all doping elements, except for Eu^{3+}, in the $NaIn_{1-x}RE_xW_2O_8$ series, beyond which concentration quenching occurs. In the case of Eu^{3+} doping, the emission intensity increases with increasing concentration from 0.03 to 0.1. The PL properties of phases with $x > 0.1$ were not studied because unidentified impurities were detected by X-ray diffraction. Usually, the concentration quenching of the emission is due to rapid migration of energy among the activator ions at high activator concentrations. During this process, the excitation energy is trapped at crystal defects and emitted non-radiatively. This leads to a decrease in the PL emission intensity [1].

4. Conclusions

This study of the PL properties of the rare-earth ion doped $NaInW_2O_8$ double tungstate shows that the phosphors exhibit a host emission close to that of $LiInW_2O_8$, but with a smaller intensity. In both oxides, doped with Dy^{3+} and Tm^{3+}, the host absorption is dominant and the energy transfer from the host to the activators (Dy^{3+} and Tm^{3+}) takes place. For Eu^{3+} doping, the host absorption is less dominant for Na-phase than for the Li-phase, but the energy transfer from the host to Eu^{3+} is more efficient for the Li-phase than for the Na-phase. In contrast, the Na-phase exhibits more efficient intra-*f*–*f* transitions of the Eu^{3+} ions. No host lattice absorption is observed for both Tb^{3+} doped Li and Na oxides, but intra-*f*–*f* emission is observed for the Na-phase, in contrast to the Li-phase which does not give any emission. Importantly, each of the phosphors of the $NaInW_2O_8$ matrix exhibits its own characteristic emission, i.e., intense red for Eu^{3+}, yellow for Dy^{3+}, blue for Tm^{3+} and green for Tb^{3+}, differently from the $LiInW_2O_8$ matrix for which only intense red and blue phosphors have been observed for Eu^{3+} and Tm^{3+}, respectively, white emission being observed for Dy^{3+}.

References

[1] G. Blasse, B.C. Grabmaier, Luminescent Materials, Springer-Verlag, Berlin, Germany, 1994.
[2] M. Yu, J. Lin, Z. Wang, J. Fu, S. Wang, H.J. Zhang, Y.C. Han, Chem. Mater. 14 (2002) 2224–2231.
[3] X. Liu, R. Pang, Q. Li, J. Lin., J. Solid State Chem. 180 (2007) 1421–1430.
[4] X. Liu, C. Lin, Y. Luo, J. Lin., J. Electrochem. Soc. 154 (1) (2007) J21–J27.
[5] Y. Chen, H.K. Yang, J.W. Chung, B.K. Moon, H. Choi, J.H. Jeong, J. Korean Phys. Soc. 57 (6) (2010) 1760–1763.
[6] Z. Wang, H. Liang, Q. Wang, L. Luo, M. Gong, Mater. Sci. Eng. B 164 (2009) 120–123.
[7] K.S. Hwang, Y.S. Jeon, S. Hwangbo, J. Tae, Opt. Appl. XXXIX (2009) 375–382.
[8] Q. Shao, H. Li, K. Wu, Y. Dong, J. Jiang, J. Lumin. 129 (8) (2009) 879–883.
[9] C. Cascales, A. Méndez Blas, M. Rico, V. Volkov, C. Zaldo, Opt. Mater. 27 (2005) 1672–1680.
[10] E.V. Zharikov, C. Zaldo, F. Diaz, Mater. Res. Soc. Bull. 34 (4) (2009) 271–276.
[11] K. Nitsch, M. Nikl, C. Barta, D. Schultze, A. Triska, R. Uecker, Phys. Status Solidi A 118 (1990) K133.
[12] V.N. Baumer, Yu.N. Gorobets, M.B. Kosmyna, B.P. Nazarenko, V.M. Puzikov, A.N. Shekovtsov, O.V. Zelenskaya, Funct. Mater. 15 (4) (2008) 537–539.
[13] M. Derbal, L. Guerbous, O. Djamel, C.J. Pierre, M. Kadi-Hanifi., Adv. Condens. Matter Phys. 2009 (2009) 327605–327612.
[14] S. Asiri Naidu, S. Boudin, U.V. Varadaraju, B. Raveau., J. Solid State Chem. 184 (2011) 2566–2570.
[15] P.N. Namboodiri, A.B. Phadnis, V.V. Deshpande., Thermochim. Acta 144 (1989) 151–157.
[16] P.V. Klevtsov, R.F. Klevtsova, J. Solid State Chem. 2 (1970) 278–282.
[17] S.P. Tandon, J.P. Gupta, Phys. Status Solidi 38 (1970) 363–370.
[18] B. Glorieux, V. Jubera, A. Apheceixborde, A. Garcia, Solid State Sci. (2000) 1–8.
[19] V. Sivakumar, U.V. Varadaraju, J. Electrochem. Soc. 153 (3) (2006) H54–H57.
[20] N. Lakshminarasimhan, U.V. Varadaraju, Mater. Res. Bull. 41 (2006) 724–731.
[21] G. Blasse, Struct. Bonding (Berlin) 42 (1980) 1.
[22] J. Hölsä, M. Leskelä, J. Lumin. 48/49 (1991) 497–500.
[23] E. Loh, Phys. Rev. 147 (1966) 332–335.
[24] I.M. Nagpure, V.B. Pawade, S.J. Dhoble, Luminescence 25 (2010) 9–13.
[25] B. Grobelna, J. Alloys Compd. 440 (2007) 265–269.